



POLITECNICO
MILANO 1863

SCUOLA DI INGEGNERIA INDUSTRIALE
E DELL'INFORMAZIONE

EXECUTIVE SUMMARY OF THE THESIS

Designing a test rig for an electrical multi-propeller system

LAUREA MAGISTRALE IN AERONAUTICAL ENGINEERING - INGEGNERIA AERONAUTICA

Author: GABRIELE MORELLI

Advisor: PROF. PIERANGELO MASARATI

Co-advisor: MICHELE ZILLETTI

Academic year: 2021-2022

1. Introduction

The design of new multi-propeller eVTOL (Electric vertical take-off and landing) aircraft configurations for Advanced Air Mobility requires both new experimental and analytical tools and studies. The relative position between LTUs (LTU stands for Lift/Thrust Unit) ¹ and their tilt angle can vary greatly between these kind of aircraft (see references [2] and [6]), and both parameters are expected to have a substantial impact on their performance, acoustics and interactional aerodynamics. Moreover, among the peculiar and critical aspects of configurations such as the tilt-propeller and tilt-wing, one is the generation of substantial dynamic, high-frequency structural loads taking place during the conversion phase, which could lead to shortened life of the aircraft structure due to fatigue, and passengers discomfort due to excessive noise and vibrations. The practical significance of designing a wind tunnel test rig in which both the relative position between LTUs and their tilt angle are adjustable, can therefore be appreciated. A notable example of such a test rig is discussed in [4]. The concept is shown in Figure 1.

¹The term "LTU" is used to denote the system comprising the propeller and the electrical motor by which it is driven. An example is shown in Figure 4

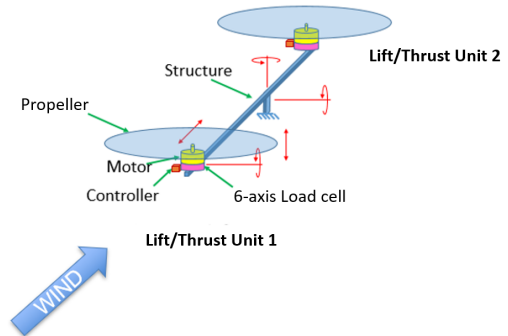


Figure 1: Wind tunnel test rig schematic diagram

In the context of this project, this thesis presents a cost-effective design of a single LTU test rig (see Figures 2 and 3) capable of measuring all the six components of its static and high-frequency (up to 250 Hz) dynamic loads and its relevant electrical parameters while simultaneously and effectively controlling its RPM (Revolutions per minute) to a sufficiently constant value. To achieve these results, several challenges had to be overcome. The first one, was indeed the design of an electrical drive system to drive the LTU RPM at sufficiently constant RPM. Among others, this required the design and programming of a custom Hall effect sensor PCB (Printed circuit board), and a de-

tailed analysis of the working mechanisms of the main components of electrical drive systems for a BPMSM (Brushless permanent magnet synchronous motor), and part of this analysis led also to a method for the preliminary choice of these main components. Another challenge was the design of a load cell-based measurement system having a dynamic behaviour suitable for measuring loads with frequency as high as 250 Hz. To this end, three load cell-based measurement systems were designed and produced, two of which turned out to be suitable. The static and dynamic loads data obtained with the different systems were then compared, both in hover and in forward flight.

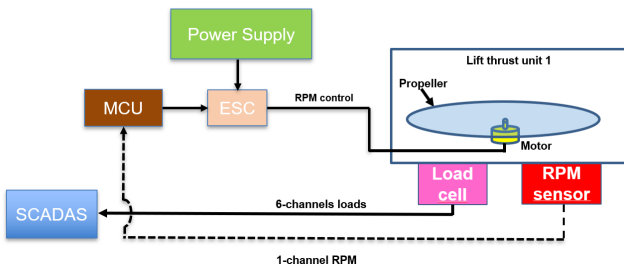


Figure 2: Functional block diagram of the single LTU test rig

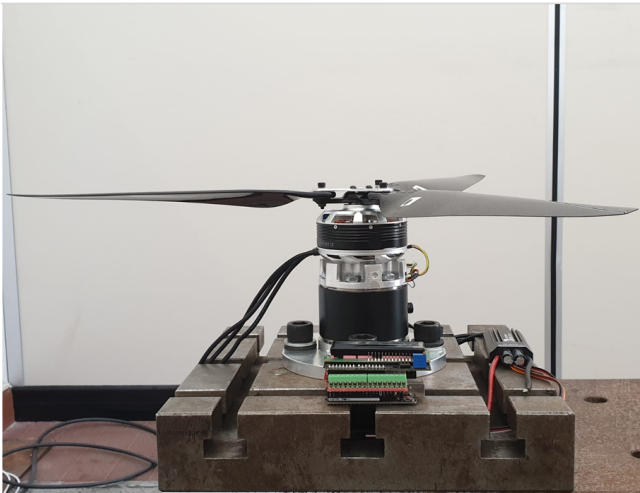


Figure 3: Single LTU test rig

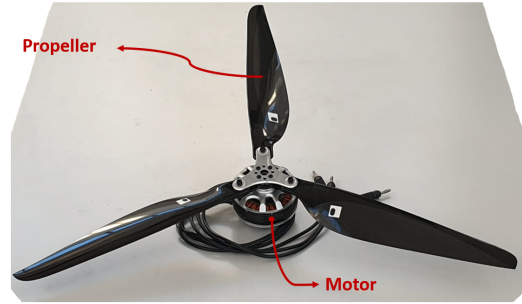


Figure 4: LTU

2. Design of the LTU electrical drive system

Referring to Figures 2 and 3, the high-level description of the electrical drive system of the final version of the test rig goes as follows. A 622.30 mm diameter triple blade propeller is driven by an 80 mm diameter BPMS motor. The ESC (Electronic speed controller), powered from a DC (Direct current) Power Supply, drives the motor when detecting PWM (Pulse-width modulation) pulses from the MCU (Microcontroller Unit). The loop could be closed by an custom Hall-based rotary magnetic RPM sensor : the MCU sets the value of the PWM duty cycle according to the RPM value measured by this RPM sensor. The motor, propeller and ESC were available from the beginning as off-the-shelf components. The detailed analysis showed, among others, that the motor RPM is directly proportional to the duty cycle of the ESC output PWM signal. However, the ESC requires a driving input PWM signal, V_{thr} (in practice the "throttle" signal), whose duty cycle is put in a linear relationship with the one of the output PWM signal actually driving the motor (see Figure 5). Moreover, the ESC does not feature any internal speed or torque controller, and no RPM sensor was available to measure the motor RPM. Therefore, it was necessary to program a MCU to both generate the signal V_{thr} and to adjust its duty cycle to control the RPM. In the end, an LCD (Liquid Crystal Display) was connected to the MCU to adjust the duty cycle of V_{thr} , and so the RPM value, by means of UP and DOWN Push Buttons. In this way an open-loop RPM control was achieved.

However, the question arises as to whether with this open-loop control scheme the RPM are "satisfactorily constant" or not, by which is meant

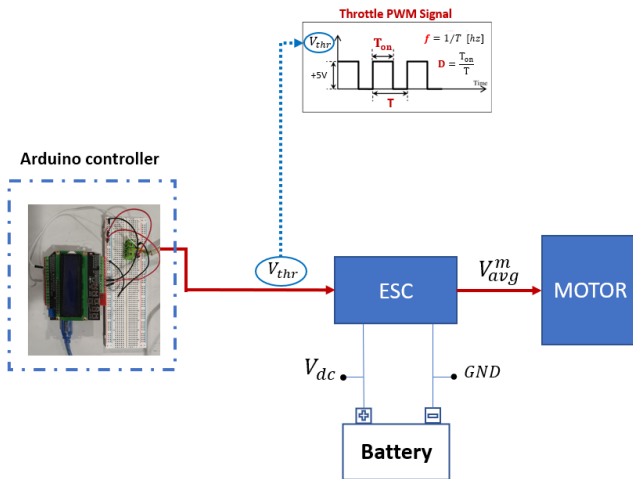


Figure 5: Open-loop voltage control scheme

that their steady-state oscillations are within 5% of the mean value. Therefore, a custom Hall effect sensor PCB was designed and produced (see Figure 7) to measure the LTU RPM. The general idea is shown in Figure 6. The sensor measures the absolute angle of a diametrically magnetized magnet (indicated with "M" in the Figure). The MCU was programmed to read the raw angle from the sensor registers, convert it to an angle in degree, and calculate the RPM by taking the difference between the current and the previous angle readings and dividing it by the time interval between the two. Once produced, the sensor was tested by comparing the average of its RPM readings to the RPM reading obtained with a microphone, and a good agreement was found between the two, with a discrepancy of less than 5% over the entire RPM/duty cycle range. Using this custom sensor, several tests were performed to measure the LTU RPM at different values of the duty cycle, and the results showed that, with the open-loop scheme proposed, the RPM were satisfactorily constant. Therefore, it was not deemed necessary for the sake of this work to program the MCU also for a closed-loop control, although the system is completely set up for closed-loop RPM control, should the latter turn out to be desirable in the future for wind tunnel measurements.

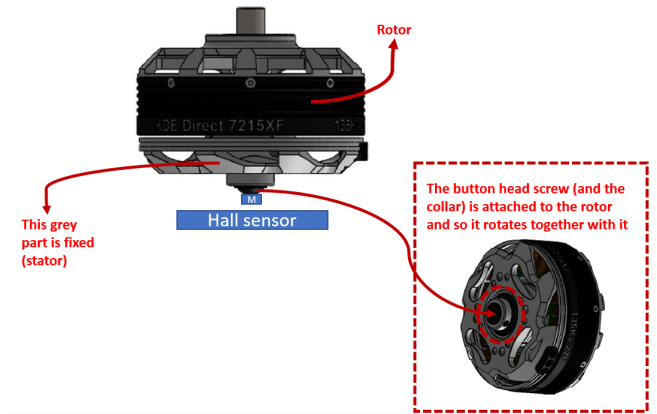


Figure 6: RPM sensor concept

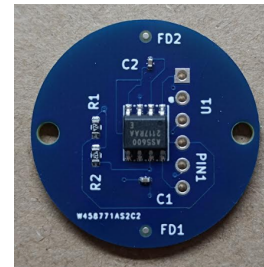


Figure 7: Hall sensor custom PCB

3. Design of the load cell-based measurement system

In order to measure all the six components of LTU dynamic loads, it was first of all necessary to design a load cell-based measurement system having a good dynamic behaviour over the entire frequency range of interest. This range was established by the objective to be able to accurately measure at least the 3/rev harmonic component of each of the six signals. The significance of the 3/rev harmonic component lies in the fact that, theoretically, it is the lowest frequency load component transmitted to the rotor shaft. In fact, under the hypothesis of identical blades performing the same periodic motion, it could be proven (see section 18.3 of reference [3]) that only the static component and components which are integer multiplies of the number of blades, 3 in our case, are transmitted to the LTU rotor shaft. Since the maximum angular speed achievable by the LTU is 5000 RPM, the maximum frequency of its 3/rev harmonic component is 250 Hz. For this reason, the frequency range [0, 250] Hz was established as the one of interest. The dynamic behaviour of a loads measurement system is defined (when it

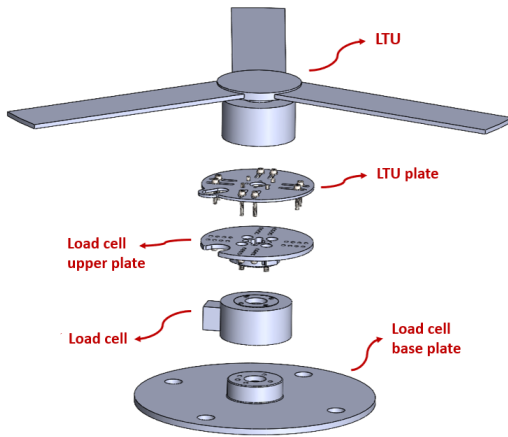


Figure 8: 6ADF80-based measurement system setup

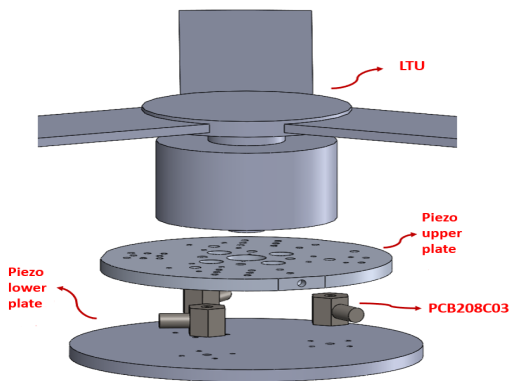


Figure 9: Piezoelectric measurement system setup

can be considered linear) by six "Frequency response functions" between the six applied, reference force/moment components and those measured by the load cell. Ideally, each of these FRFs ("Frequency response functions") should be of unit magnitude and zero phase over the entire frequency range of interest. For reasons stated below, three alternative load cell-based measurement systems were designed and produced, but all these three solutions feature an off-the-shelf load cell (or multiple off-the-shelf load cells) and a mechanical interface between the motor and the load cell. The CAD assembly models of the three systems are shown in Figures 8, 9 and 10, and the last designed system can also be seen in Figure 3. Two out of the three systems are based on two different 6-axis strain gauge load cells, and one is instead based on three uniaxial piezoelectric load cells. From the point of view of the frequency response, the best kind of commercially available

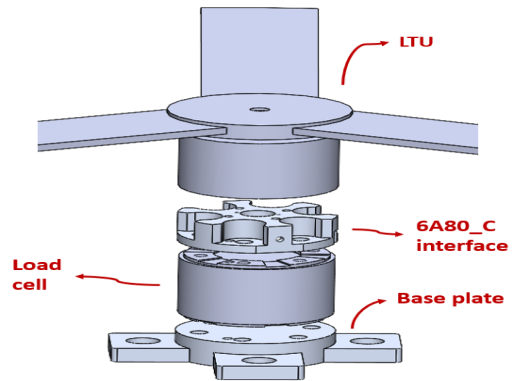


Figure 10: 6A80C-based measurement system setup

load cell to measure the six components of dynamic loads is a 6-axis piezoelectric load cell, but due to the design objective of keeping the overall design cost low, comparatively low cost parts like the two six-axis strain gauge load cells and the three uniaxial piezoelectric load cells were tentatively chosen. The risk associated with the six-axis strain gauge load cells was that only their static characteristics in the form of a static calibration matrix were provided by the manufacturer. In fact, no experimental data was available to prove the suitability of their frequency response in the frequency range of interest. Similarly, although the single uniaxial piezoelectric load cell has a very good frequency response for our purposes, the presence of mechanical interface, for example, could have a negative impact on the frequency response of the overall measurement system. Therefore, in all three cases it was necessary to test for the measurement system frequency response. To this end, the systems were forced in multiple directions with an electrodynamic shaker. The idea is shown in Figure 11. In some cases, whenever further investigations were necessary, a hammer test was also performed.

The first challenge in designing these systems was the design of the mechanical interface. In fact, the following design constraints must be fulfilled:

- The interface's first mode frequency must be sufficiently higher than that of the load cell
- It has to be as lightweight as possible
- It has to be as compact as possible

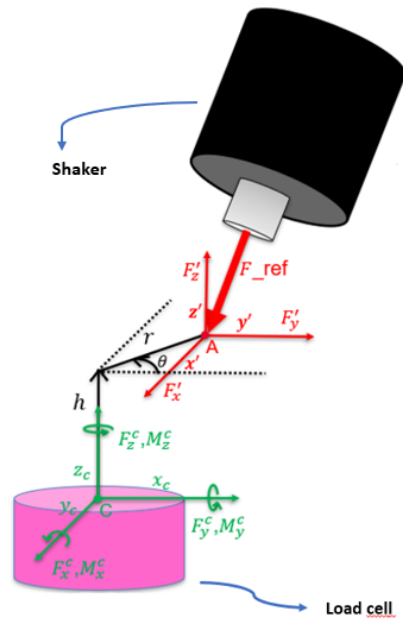


Figure 11: Measurement system test setup

- Multiple attachment points for the shaker stinger must be present

The second challenge was devising a shaker test setup. Figures 12 and 13 show the shaker setup which was adopted throughout this thesis work. The system is excited by an electrodynamic shaker which is either suspended or attached to a very rigid block. To measure the force applied by the shaker during the test, an uniaxial piezoelectric load cell is placed in series with the shaker stinger, and the whole system stinger+load cell threaded into the forcing point either on a rectangular shaped part or on the mechanical interface itself. The shaker input open-loop control signal is generated by the Siemens SCADAS data acquisition system and then fed to an amplifier connected in series and before the shaker. To derive the FRFs between the reference and the measured force/moment components, a “Stepped Sine Test” was performed. In this test, the frequency of the shaker excitation force is increased (up cycle test) or decreased (down cycle test) at a given frequency step (see reference [5]). The SCADAS generates a sinusoidal waveform at a given frequency, and after a certain settling time is elapsed, it then calculates the FRF between the shaker reference (excitation) force F_{ref} (see Figure 11) and each channel non-

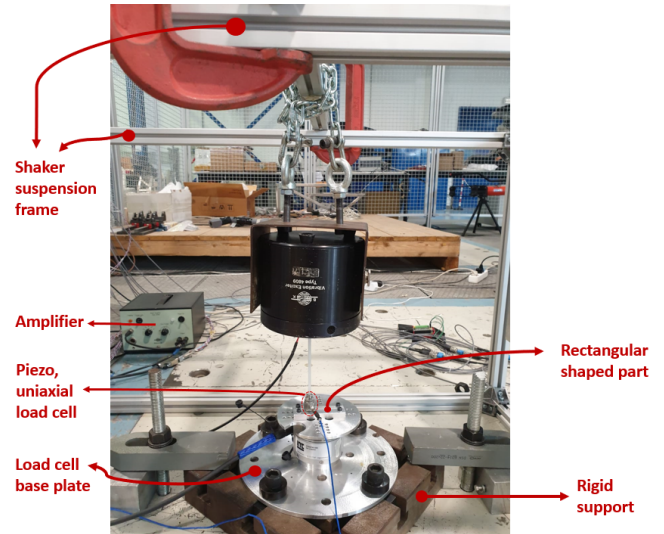


Figure 12: Shaker test setup

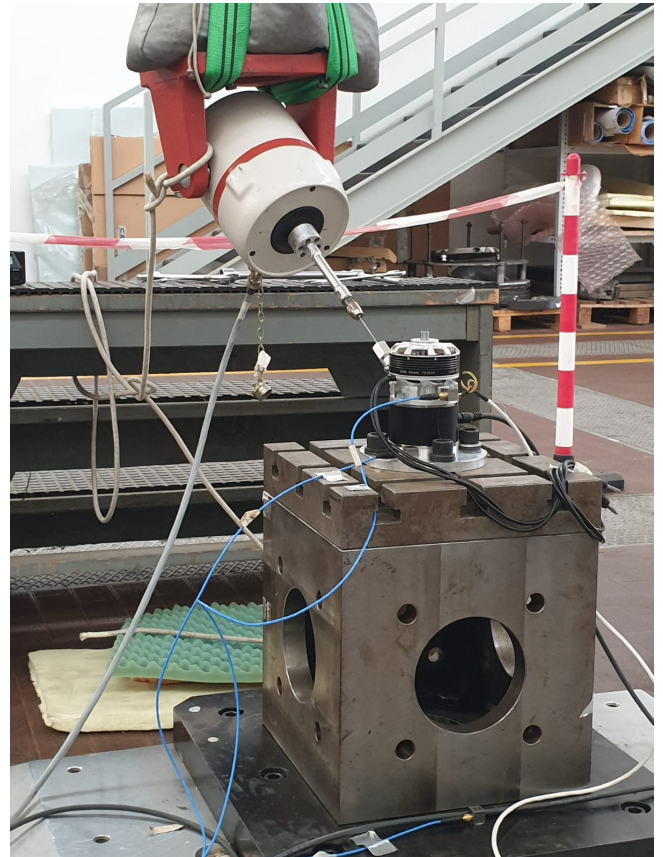


Figure 13: Shaker test setup, out-of-plane excitation force

dimensional voltage signal ². The force/moment components FRFs (an example of which is shown in Figure 14 for the M_Y moment component) are then computed in post-processing either by using the load cell static calibration matrix or geometrical relationships (as in the case of the piezoelectric system). To assess the FRF data computed by the SCADAS, the FRFs of the channels were also computed in Matlab, starting from the time histories of F_{ref} and those of the channels non-dimensional voltages, by computing the channels average autopower spectra and the average cross power spectra between each channel and F_{ref} (see section 3.5 of reference [1]). The results of the shaker tests on the first measurement system showed a structural resonance at around 110 Hz associated with the load cell. As an example, the FRF of the M_Y moment component is reported in Figure 15. Therefore, the load cell frequency response is not suitable for the application, for which a bandwidth of at least 250 Hz is required, although the system is capable of measuring the six components of static loads (see section 4). In view of these results, the piezoelectric system was designed, which instead showed a suitable frequency response. As an example, the FRF of the M_Y moment component is reported in Figure 14. It turned out that the dynamic at 200 Hz is a highly damped (around 20% damping ratio) resonance associated with the motor, which is not part of the measurement system, being instead part of the LTU, i.e. of the subsystem whose dynamic characteristics are the measurement objective. On the other hand, the more prominent dynamics between 450 and 600 Hz are associated with the upper plate (see Figure 9) or with a combination of upper plate and motor. With its three vertically arranged uniaxial load cells (see Figure 9), this setup can only measure the vertical force component (thrust), and the two out-of-plane moment components. This limitation could be overcome, and the frequency of the upper plate dynamics further increased, by substituting the three uniaxial piezoelectric load cells with four symmetrically placed triaxial piezoelectric load cells. At this point, the supplier of the first tested load cell made themselves

²The channels are six and three, respectively, in the case of the two measurement systems based on a 6-axis load cell, and in the case of the piezoelectric system

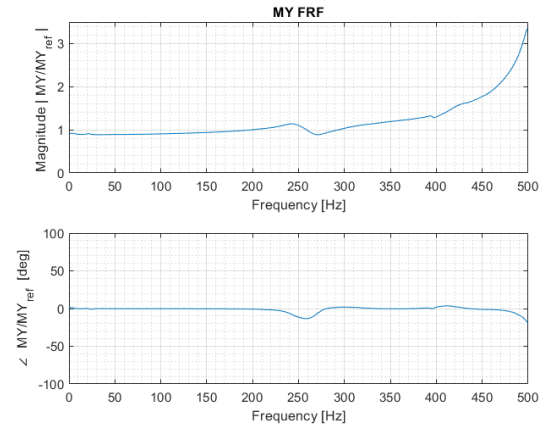


Figure 14: FRF of M_Y , piezoelectric system

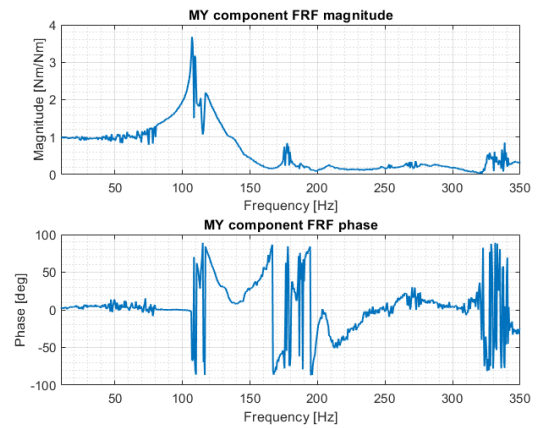


Figure 15: FRF of M_Y moment component, 6ADF80-based system

available to lend a different 6-axis strain gauge load cell, in order to test its dynamic characteristics. The rationale behind this proposal was that an in-house FEM (Finite element method) model of the load cell yielded a frequency for its first structural mode of roughly 800 Hz. Therefore, the measurement system shown in Figures 10 and 3 was designed. The results of the tests yielded a value of roughly 700 Hz for the load cell resonance frequency, and a 500 Hz resonance peak associated to the foundation (possibly to the "Base plate" shown in Figure 10). In general, the test results show that this measurement system is capable of measuring all the six components of dynamic loads in the [0 250] Hz frequency range of interest.

4. Measuring LTU loads

Several tests were performed to measure the magnitude of both the static and dynamic con-

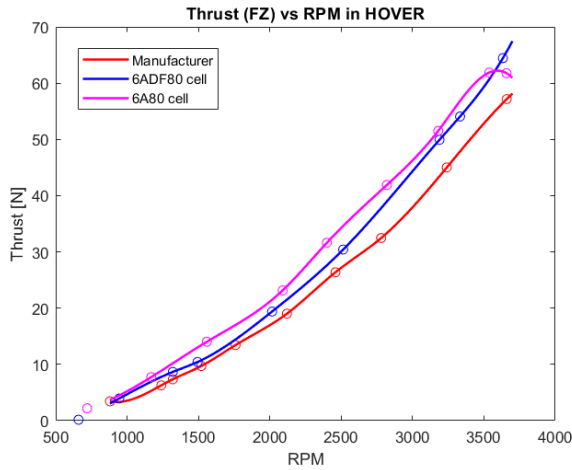


Figure 16: LTU static thrust comparison

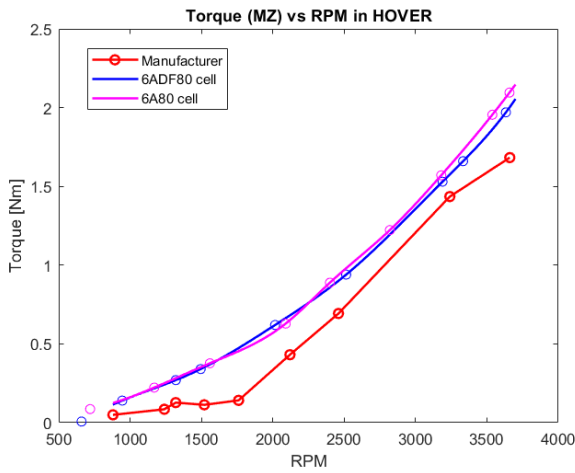


Figure 17: LTU static torque comparison

tributions of the LTU force/moment components, both in "Hover flight condition" and in "Forward flight condition", which was crudely simulated by means of a fan delivering an air-flow of 32.5 km/h. In each test the LTU loads were measured at a given RPM value, which was set by setting the value of the PWM duty cycle via the LCD display. Figures 16 and 17, show a comparison between the static components of thrust (F_Z) and torque (M_Z), respectively, measured with the six-axis strain gauge load cells (6ADF80 and 6A80C systems), and those measured by the LTU supplier. The relatively small discrepancy between the 6ADF80 and the 6A80C results is likely due to the different distances of propeller from ground and to different air conditions.

In Figure 18 some F_Z (thrust) magnitude spectra in hover obtained with the piezoelectric sys-

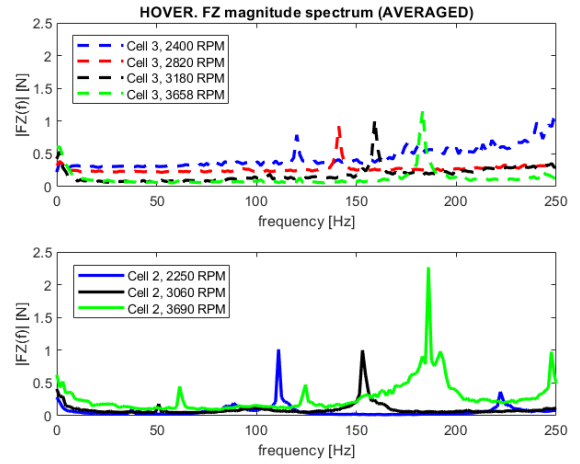


Figure 18: Comparison between Piezo (cell 2) vs 6A80C (cell 3) magnitude spectra

tem (indicated by "Cell 2" in the Figure) are compared with some spectra obtained with the 6A80C based system (indicated by "Cell 3". This is the one with a suitable frequency response) at different but comparable RPM values, and the comparison is successful.

5. Conclusions

In this thesis, a cost-effective, single LTU test rig capable of driving the LTU at constant RPM and of measuring all the six components of static and dynamic loads in the 250 Hz frequency range was presented. It was shown that, with the given ESC, a satisfactory open-loop control can be achieved by programming a relatively simple MCU, and that a custom, programmable Hall sensor PCB is a relatively simple and cost-effective option to implement a closed-loop RPM control. It is deemed necessary, especially in view of the possible need of programming the MCU for a closed-loop RPM control for wind tunnel measurements, to further assess the precision and bandwidth of the designed RPM sensor. In view of the future use of the test rig for wind tunnel measurements, the electrical drive system presented in this work could be used to either simultaneously or independently control the RPM of multiple LTUs. Furthermore the wind tunnel control system for the tilt angle should be assessed and possibly incorporated in the electrical drive system to finally obtain a basic flight controller. The static loads were measured and the thrust and torque compo-

nents were found to be in very good agreement between the different measurement systems designed and the LTU manufacturer. As far as dynamic loads are concerned, it was concluded that the piezoelectric and the 6A80C-based system are both suitable to measure loads in the specified frequency range provided that the support they are mounted on responds dynamically only at a sufficiently high excitation frequency. This latter assumption is particularly important again in connection to the future use of the test rig for wind tunnel measurements. In fact, the dynamic characteristics of the structure in the wind tunnel supporting the LTUs will have to be at least comparable with those of the supporting structures considered in this work. Moreover, the magnitude spectra of the loads obtained with the piezoelectric system compare successfully (the representative case of thrust was reported) in the specified frequency range to those obtained with the 6A80C-based system. The number of load components the piezoelectric system is able to measure could be extended from three to all six by replacing, for example, the three uniaxial piezoelectric load cells with three, or better four triaxial piezoelectric load cells.

6. Acknowledgements

First of all, I am very appreciative of Michele Zilletti of Leonardo Helicopters for his professional, timely and useful advice during all this thesis work. Then, I would like to thank Professor Masarati for giving me the opportunity to work on this project, and Davide Marchesoli, Andrea Zanoni and Mauro Terraneo for their collaboration on the data acquisition phase. I would also like to thank Giovanni Chiarolla for taking interest in this project, and last but not least Paolo Rubini, Roberto Bertè for the manufacturing work, and Alessandro Mottironi for part of the electrical work.

References

- [1] Robert E. Coleman. *Experimental structural dynamics*. AuthorHouse, 2004.
- [2] UBER Elevate. Fast-forwarding to a future of on-demand urban air transportation. Technical report, UBER Elevate, 2016.
- [3] Wayne Johnson. *Rotorcraft Aeromechanics*. Cambridge University Press, 2013.
- [4] Carl Russell and Sarah Conley. The multi-rotor test bed – a new nasa test capability for advanced vtol rotorcraft configurations. Technical report, NASA, 2020.
- [5] SIEMENS. Multi input multi output mimo testing. SIMCENTER - TESTING, 2020.
- [6] Alex Stoll and JoeBen Bevirt. Development of evtol aircraft for urban air mobility at joby aviation. Technical report, Joby Aviation, 2022.